LP01

Differential phase contrast electron microscopy with an A-B effect phase plate

[1]Hirohisa Niimi, [1]Uki Ikeda, [2]Takayoshi Tanji, [3]Jiro Usukura

[1]Graduate School of Engineering, Nagoya University, [2]EcoTopia Science Institute, Nagoya University, [3]Graduate School of Science, Nagoya University

[1, 2, 3] Furo-cho, Chikusa-ku, Nagoya, Japan

Observations of week phase objects, such as thin films of light elements, thin polymer films, biological sections etc., are available by electron phase microscopy[1]. Many types of phase plates have been proposed and utilized. Some electrostatic types have been developed, but they are not so general, because the fabrication of the filter with fine structures is very difficult. The mainstream of todays phase plate is a thin film type. This type of the phase plate, however, has some disadvantages, i.e. difficult control of the film thickness, charging up, contamination and so on. We adopted the phase plate with a magnetic thin filament which generates the vector potential around itself by an Aharonov-Bohm (A-B) effect. The filament type phase plate with the A-B effect was proposed and constructed firstly by Nagayama [2]. This type of the phase plate generates the differential phase contrast in the image, and has a longer life time than the thin film type. Any clear differential effect, however, has scarcely reported so far.

We will report that the effect of a phase plate consisting of a Wollaston platinum filament of 1μm in diameter covered with ferromagnetic material, Nd-Fe-B of 5 nm thick, deposited by Pulsed Laser Deposition. The filament with a clean surface selected by SEM is mounted on a single hole Cu grid. The phase difference between both sides of the filament measured by electron holography shows 1.5 rad. Being set on the aperture holder, the phase plate is inserted in the back focal plane of the objective. Fig. 1 shows images of mouse photo receptor cell's inner segments fixed in osmium without stained. Fine structures can be observed clearer in the image using the phase plate than in the image taken ordinarily. The direction of the differentiation is shown by the arrowhead.

Reference

[1]K. Nagayama, Another 60 years in electron microscopy: development of phase-plate electron microscopy and biological applications, Journal of Electron Microscopy, **60** (2011) S43-S62.

[2]K. Nagayama, Development of phase plates for electron microscopes and their biological application, European biophysics journal, **37** (2008) 345-358.

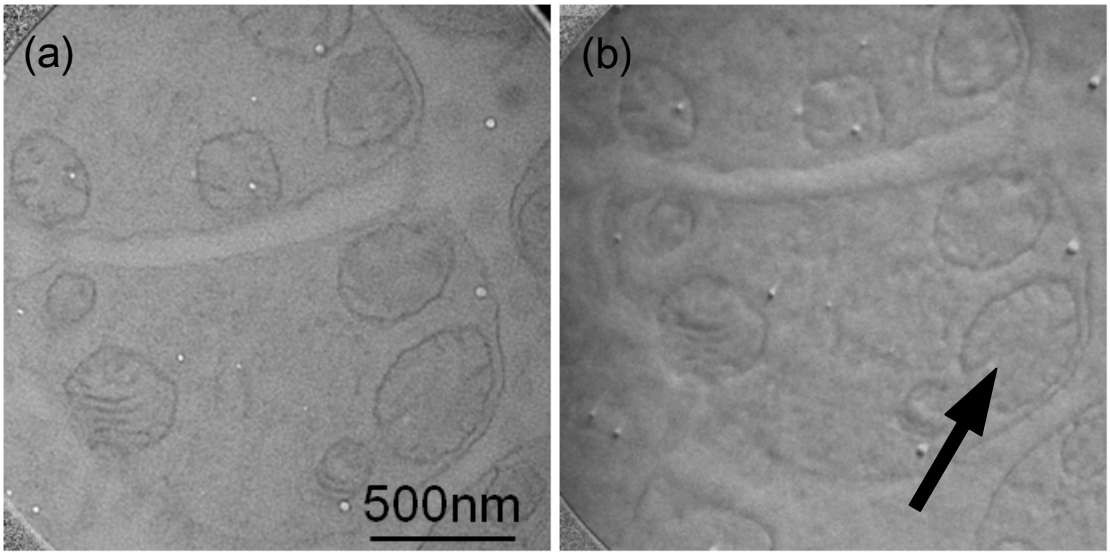

Fig. 1 TEM images of mouse photoreceptor cell's inner segments fixed in osmium taken at under-focus without the filament (a), and in-focus with the filament (b).

LP02

Fabrication and characterization of epitaxial Au/Co core-shell nanoparticles

[1]Yuta Matsushima, [2]Kazuhisa Sato, and Toyohiko J. Konno

[1]Department of Materials Science, Tohoku University, [2]Institute for Materials Research, Tohoku University

[1] Aoba-yama, Aoba-ku, Sendai 980-8579, Japan, [2] 2-1-1Katahira, Aoba-ku, Sendai 980-8577, Japan.

Metallic nanoparticles have been actively studied due to their excellent properties such as catalytic activities, magnetic, or magnetotransport properties. Phase separation is a way to control structure and properties of such bimetallic nanoparticles. Recently, novel two-phase structures were found in Au/Co nanoparticles produced by sequential electron-beam deposition. Thin Au-shell structure may have a potential to nanocatalyst applications. In this study we hence intend to characterize microstructures of the Au/Co nanoparticles and their evolution on annealing in order to clarify the thermal stability of core/shell structures.

Bimetallic Au/Co nanoparticles were fabricated by sequential electron-beam depositions of Au, Co and Al_2O_3 onto NaCl(001) substrates kept at 520 K. Particle size was adjusted by controlling the deposited thickness. Postdeposition annealing was performed at 800 K for 3.6 ks or 21.6 ks. The structure and morphology of the nanoparticles were characterized using FEI TITAN80-300, JEOL JEM-3011, and JEM-ARM200F (S)TEM.

Figure 1(a) shows a HAADF-STEM image of Au/Co nanoparticles with the average particle size of 7 nm (Au-52at%Co). Formation of core-shell structure (Au-shell) is clearly seen due to the large atomic number difference between Co and Au. According to the statistics, about 70% of the particles showed the Au-shell structure. It was found that particle size reduction is effective to produce Au-shell nanoparticles. Figure 1 (b) shows an SAED pattern of Au/Co nanoparticles. The cube-on-cube orientation epitaxy is seen between Au and fcc-Co. Figure 1(c) shows an atomic resolution HAADF-STEM image of a Au-shell/Co-core nanoparticle. Such a Au-shell structure was maintained after annealing at 800 K for 21.6 ks. It is presumed that lower surface energy of Au than that of Co is responsible for the Au-shell formation.

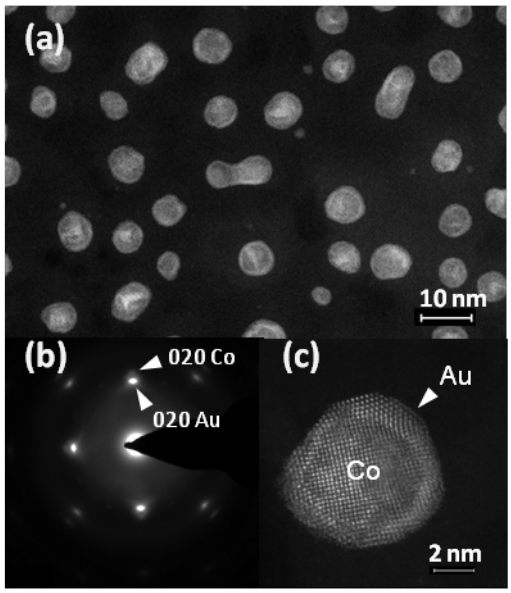

FIG. 1. (a) HAADF-STEM image of Au/Co nanoparticles, (b) SAED pattern and (c) a typical example of atomic resolution Z-contrast image of a Au-shell nanoparticle.

This study was partially supported by the Grant-in-Aid for Scientific Research (B) (Grant No. 26286021) from the Ministry of Education, Culture, Sports, Science and Technology.

LP03

Strain measurement of Heteroepitaxial GeSn/Ge microstructures by nano-beam electron diffraction

Kentaro Doi[a], Koh Saitoh[b], Nobuo Tanaka[b], Sinichi Ike[a,c], Osamu Nakatsuka[a], and Shigeaki Zaima[a]

[a]Graduate school of Engineering , Nagoya University, Japan
[b]Institute of EcoTopia Science , Nagoya University, Japan
[c]Research Fellow of the Japan Society for the Promotion of Science, Japan

The performance enhancement of large scale integration (LSI) has been achieved by a miniaturization of metal-oxide-semiconductor field effect transistors (MOSFETs) and strained Si technology for the last decade. Recently, the gate length of MOSFET reaches 20nm. These technologies are approaching to limit and, other materials substituting for Si are expected. Uniaxial compressive strained Ge, which has a larger hole mobility than strained Si, is one of the candidates to overcome the limit. Ike *et al.* made a micro-stripe structure of Ge in which uniaxial compressive strain is introduced by epitaxiral growth of a GeSn layer on the Ge substrate. They measured strain of the micro-stripes (fin) of Ge by x-ray microdiffraction. However, the strain distribution in the fin has not been measured yet. In this study, we applied nano-beam electron diffraction (NBD) to measure the strain distribution in the fins of the Ge micro-structure.

A micro-stripe structure of a Ge substrate was prepared by anisotropic wet etching. A GeSn layer was epitaxially grown on the substrate by molecular beam epitaxy (MBE). Post deposition annealing was performed at 300~600℃ for 30 min in N_2 ambient [1]. Fig.1 shows a schematic diagram of the stripe structure. Ge fins are sandwiched by GeSn layers which are epitaxially grown on both sides of the Ge fin. Composition of the Sn is 6.5%. Cross section samples were prepared by using a focused- ion- beam (FIB) instrument. The NBD experiment was conducted using a TEM operated at an acceleration voltage of 200kV. The probe size of NBD was about 15nm in diameter. NBD patterns were taken at an incidence along the [110] orientation and recorded by a 16 bit CCD camera with 2k×2k pixels. The NBD probe was scanned (two dimensional) with a pitch of 8nm and 56 diffraction patterns in total were acquired. Lattice parameters were determined by fitting the spot positions between a simulated NBD pattern which is calculated with lens distortion and experimental NBD pattern.

Fig.2(a) and (b) show strain distribution of $\varepsilon_{[110]}$ and $\varepsilon_{[001]}$ in the Ge fin respectively, overlaid on the cross-section TEM images. Tetragonal symmetry is assumed for the strained lattice ($a = b \neq c, \alpha = \beta = \gamma = 90°$) in the present study. In the present NBD analysis shows compress strains in the [$1\bar{1}0$] direction, and tensile strains in the [001] direction. Both strains are relaxed in the top of the Ge fin. Compress strains decrease with the distance from the top of the fin, and tensile strains in the [001] direction shows a maximum in the middle of the fin. The maximum values of compress strains and tensile strains are 0.66% and 0.83%, respectively. Strain values measured by x-ray diffraction were 1.35% compress strain and 0.8% tensile strain [1]. The strain values measured by the present study and x-ray are comparable in the [001] direction, whereas those in the [110] direction shows a discrepancy. The reason of the discrepancy between the results by NBD and X-ray will be discussed.

The authors are grateful to Dr. Y. Moriyama from GNC/AIST for providing the Ge micro-fin samples. This research is partially supported by by JSPS Grant-in-Aid for Scientific Research (S) (26220605) and by the JSPS through the FIRST Program initiated by CSTP.

Reference

[1] S. Ike, *et al*. *ECS Trans.*,**58**(9) 185-192(2013).

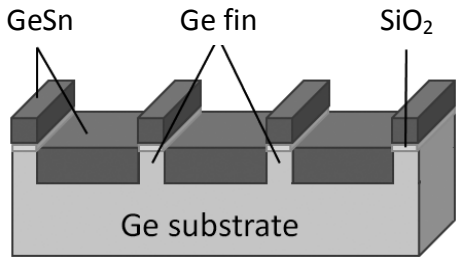

Fig.1 Schematic diagram of GeSn/Ge microstructure.

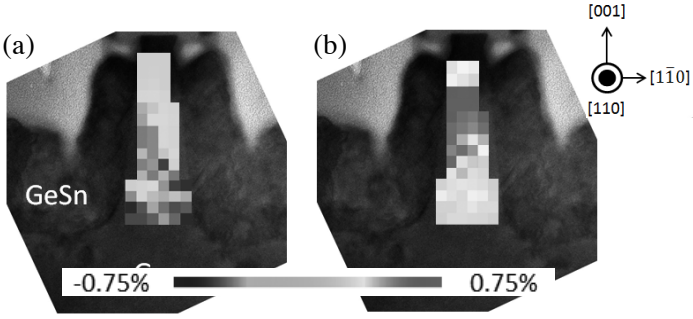

Fig.2 Cross-section TEM image piled strain distribution (a) [$1\bar{1}0$] direction strain (b) [001] direction strain